Proteomic Analysis of Differentially Expressed Proteins in Human Lung Cells Following Formaldehyde Treatment

Yu-Mi Jeon[1], Jae-Chun Ryu[2] & Mi-Young Lee[1]

[1]Department of Biotechnology, SoonChunHyang University, Asan, Chungnam 336-600, Korea.
[2]Cellular and Molecular Toxicology Laboratory, Korea Institute of Science and Technology, Seoul 130-650, Korea.
Correspondence and requests for materials should be addressed to M. Y. Lee (miyoung@sch.ac.kr)

Abstract

Chronic formaldehyde inhalation studies have suggested its relativity to teratogenicity, cancer incidence, neurodegenerative and vascular disorders. Many toxicological data on the formaldehyde toxicity are available, but proteomic results showing complete protein profiles are limited. Therefore, alterations of protein expression patterns upon formaldehyde treatment were investigated in the human lung epithelial cell line. Differentially expressed proteins following formaldehyde treatment were analyzed on 2-dimensional gels, and further analyzed by MALDI-TOF to identify the proteins. Among the identified proteins, 24 proteins were notably up-regulated and 6 proteins were down-regulated. In particular, cytoskeleton related protein named vinculin and Rho GDP dissociation inhibitor which plays a key role in apoptosis increased remarkably.

Formaldehyde is a colorless, flammable, strong-smelling gas that is produced worldwide on a large scale to manufacture building materials and produce many household products[1]. Formaldehyde is a typical Volatile Organic Compound (VOC) which received much attention as a chemical irritant responsible for sick house syndrome. Formaldehyde is also used directly in aqueous solution (formalin) as a disinfectant and preservative in many applications. In the atmosphere, formaldehyde is produced by the action of sunlight and oxygen on atmospheric methane and other hydrocarbons. Formaldehyde is an eye, skin, and respiratory tract irritant. Inhalation of vapors can produce narrowing of the bronchi and an accumulation of fluid in the lungs[2]. It also has been observed to cause cancer, namely leukemia, sinonasal cancer and cancer at other sites, including the oral cavity, hypopharynx, pancreas, larynx, lung and brain in laboratory animals and humans[3-6]. Formaldehyde has been classified as a human carcinogen by the International Agency for Research on Cancer[1], although the specific mechanism by which formaldehyde induces several types of cancer in humans is largely unknown.

More than 90% of inhaled formaldehyde is absorbed in the upper respiratory tract and it is also absorbed in the nasopharynx, trachea and proximal regions of the major bronchi. Absorbed formaldehyde can be oxidized to formate and carbon dioxide or may be incorporated into biological macromolecules via tetrahydrofolate-dependent one-carbon biosynthetic pathways[7,8]. The systemic effects of formaldehyde are due primarily to its metabolic conversion to formate and may include metabolic acidosis, circulatory shock, respiratory insufficiency, and acute renal failure[9]. Formaldehyde probably elicits airway inflammation associated with asthma through hypersensitivity and irritant mechanism[10]. Moreover, formaldehyde is one of the common causes of contact dermatitis and is thought to act as a sensitizer on the skin[11].

Formaldehyde showed dose-dependent cytotoxicity and loss of glutathione[12]. Altered Ca^{2+}-homeostatis and impairment of mitochondrial function occurred in the formaldehyde-induced cytotoxicity. Thiols, such as glutathione, and alcohol dehydrogenase 3 were involved in the protection against cell damage by formaldehyde[13].

Studies in humans, rats and monkeys revealed increased DNA-protein cross-links following exposure to formaldehyde[14-16]. Especially both genotoxicty and cytoxicity played important roles in the carcinogenesis of formaldehyde in nasal tissues. The current data indicate that DNA-protein cross-links provide a potentially useful marker of genotoxicity, while the data on the total protein profiles related with the genotoxicity and cytotoxicity are much more limited[17-19]. Therefore, large-scale, high-throughput, whole-proteomic studies are needed to understand the genotoxicity and cytotoxicity by formaldehyde.

The levels of mRNAs do not necessarily predict the

levels of the corresponding proteins in a cell, even if gene microarrays offer the expression of many or all genes in a cell. Although genomics cannot explain post translation modification, proteomics can determine the global protein changes in a cell. Furthermore, the development of proteomic techniques facilitates the elucidation of the protein functions under stress condition, resulting in the discovery of bio-
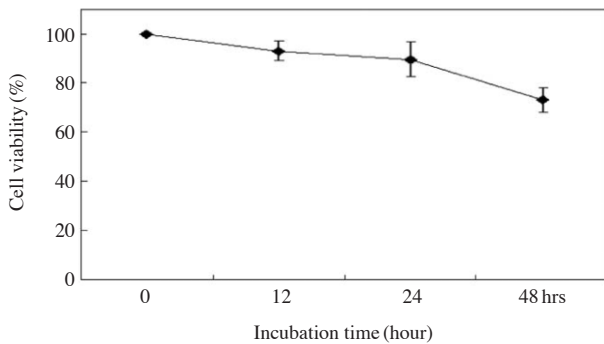
markers in response to environmental toxicity[20]. To better understand the cytotoxicity and to develop a protein marker candidate for formaldehyde-induced cytotoxicity, proteomic analysis of differentially expressed proteins in the human lung cells by formaldehyde was performed.

Cytotoxicity of Formaldehyde in Human Lung Epithelial Cells

Cell viability of human lung epithelial cells after treatment of 100 μM formaldehyde at different exposure times was determined by MTT assay. Formaldehyde reduced the viability of the cells in a time-dependent mode. As shown in Figure 1, exposure of 100 μM formaldehyde for 48 hrs resulted in approximately 30% non-survival of the cells. This concentration and exposure time were considered to be acceptable for conducting proteomic analysis.

Proteomic Identification of Differentially Expressed Proteins after Formaldehyde Treatment in Human Lung Epithelial Cells

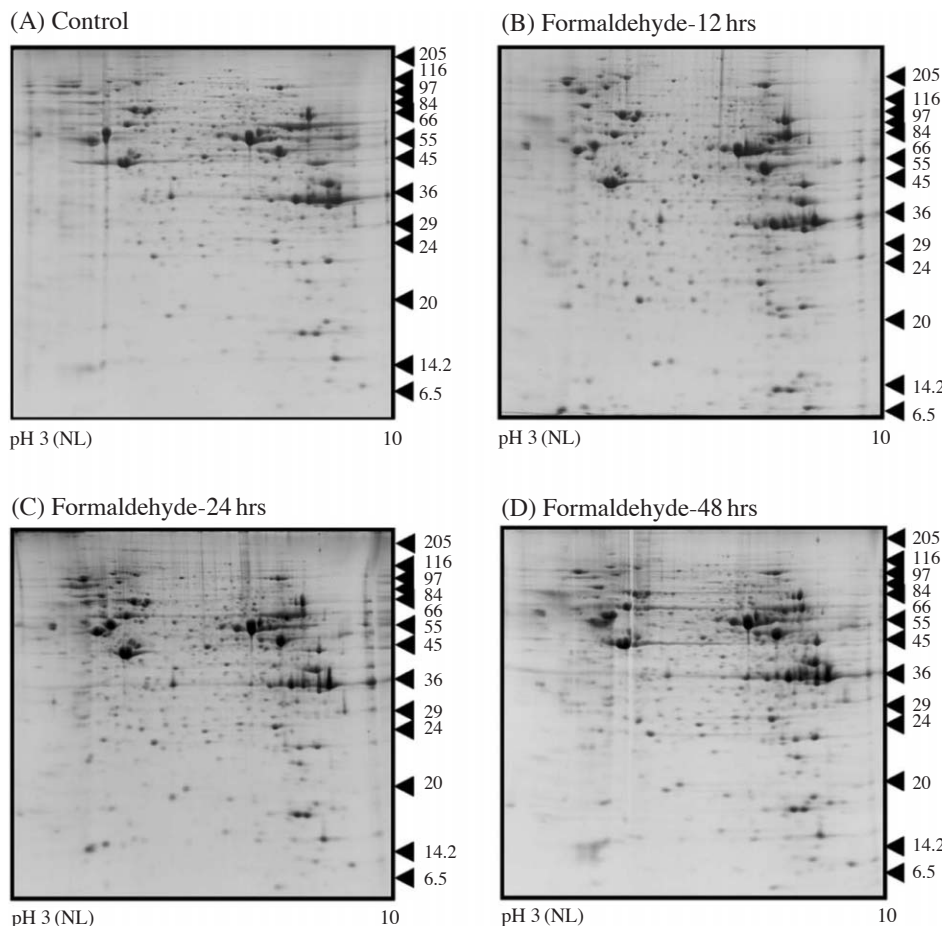To study the differential expression of proteins in

Figure 1. Cell viability tests of human lung epithelial cells after formaldehyde treatment by using MTT assay.

(A) Control

(B) Formaldehyde-12 hrs

(C) Formaldehyde-24 hrs

(D) Formaldehyde-48 hrs

Figure 2. 2-DE images showing the protein spots from control and formaldehyde-treated human lung epithelial cells for 0, 12, 24 and 48 hrs.
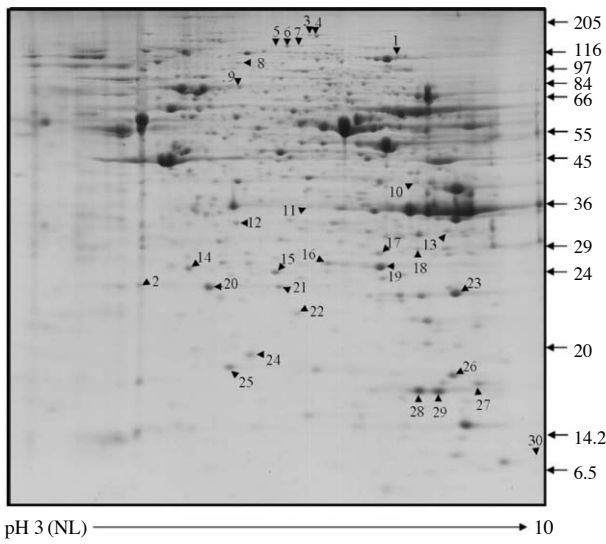
Figure 3. Master gel image showing the separation of total proteins from human lung epithelial cells.

lung cell after formaldehyde treatment, proteomic analysis was performed using high-resolution 2-DE. Figure 2 shows 2-DE images of the liver proteins following treatment of 100 μM formaldehyde for 0, 12, 24 and 48 hrs. Figure 3 is a representative master gel image showing the separation of human lung cell proteins. More than 350 protein spots with pIs between 3 and 10 and with relative molecular masses between 6.5 and 205 kDa were detected on the 2-DE gels. In order to preselect proteins exhibiting variations in expression levels, the proteins from treated sample and untreated control were compared by using ImageMaster 2-DE gel analysis software. After comparing the 2-DE protein patterns on duplicate gels of lung cell, we found 30 protein spots that were significantly different after formaldehyde treatment. Among them, 24 spots marginally increased at 48 hrs of 100 μM formaldehyde treatment (Figure 4) and 6 spots were decreased (Figure 5).
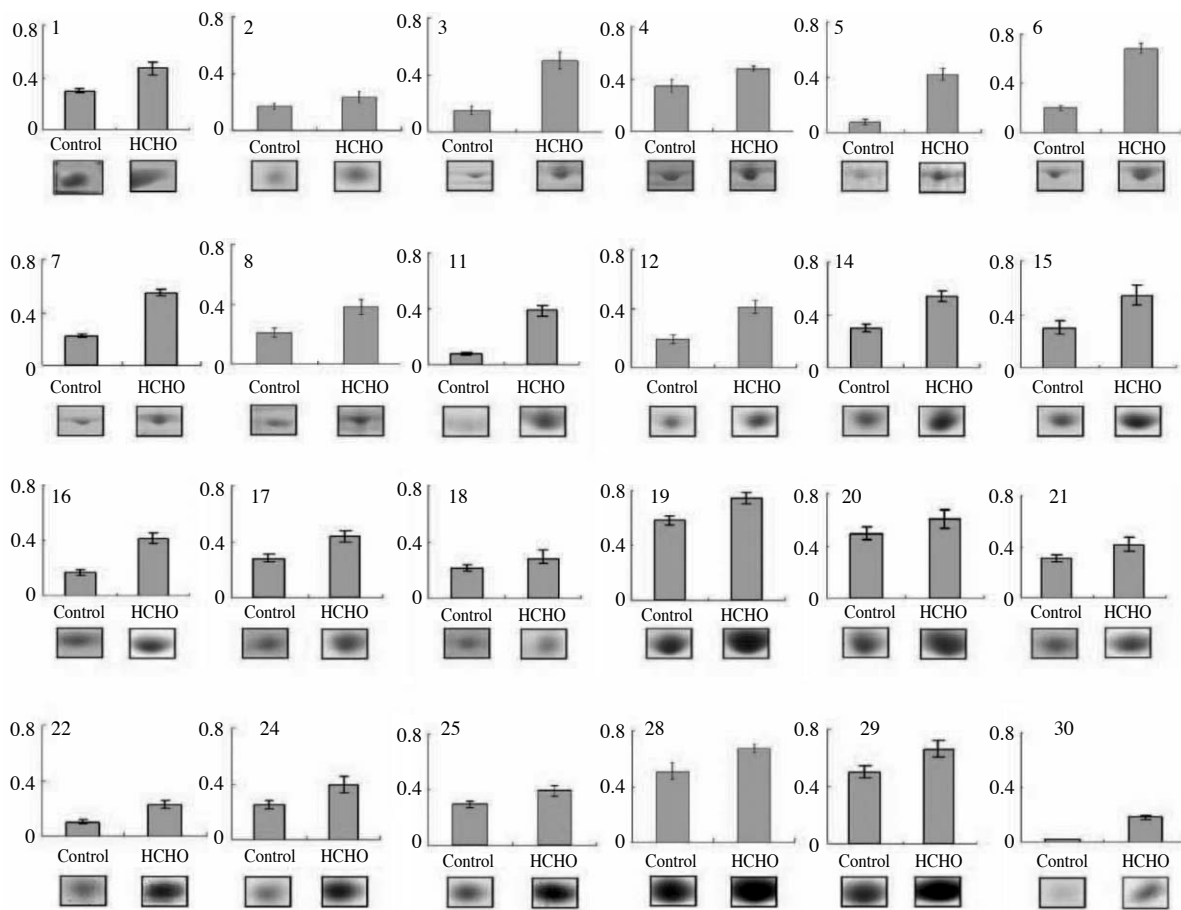
The protein spots that revealed statistically signifi-

Figure 4. Up-regulated proteins from human lung epithelial cells by formaldehyde. Protein expression levels were determined by relative intensity using image analysis.

Figure 5. Down-regulated proteins from human lung epithelial cells by formaldehyde. Protein expression levels were determined by relative intensity using image analysis.
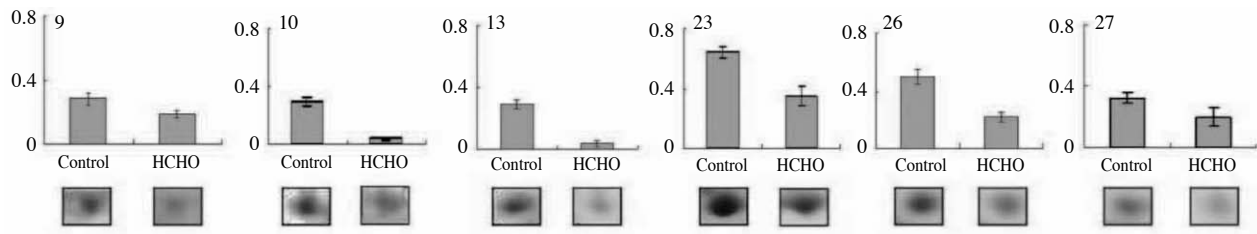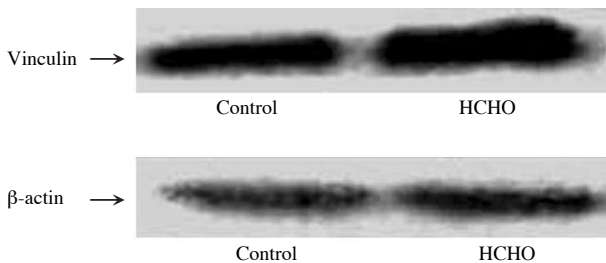

Figure 6. Western blot analysis of vinculin in human lung epithelial cells following formaldehyde treatment.

cant differences were excised from the gels, trypsinized, and analyzed by MALDI-TOF MS. The number of matching peptides, the percentage of sequence coverage, and the accuracy of mass estimates were used to evaluate the database search results and hence, 30 proteins were identified (Table 1). Interestingly, cytoskeleton related vinculin increased remarkably, and Rho GDP dissociation inhibitor which plays a key role in apoptosis was also up-regulated.

Western Blot of Vinculin Protein

To confirm whether the up-regulation of vinculin expression can also be detected by immunological method, we performed western blot analysis (Figure 6) using vinculin-specific antibody. The result indicated that the vinculin protein was expressed at low level in normal lung cell, but was present at considerably higher levels after formaldehyde treatment. These results substantiate the specific up-regulation of vinculin expression in the lung epithelial cell after formaldehyde treatment.

Discussion

The differentially expressed proteins in human lung epithelial cells after formaldehyde treatment were investigated through proteomic approaches. To avoid experimental variation and obtain statistically significant changes in protein levels, three replicate gels from the same sample were used here. 30 protein spots that were differentially expressed after formaldehyde treatment were found on the 2-DE gel. Among them, 24 spots were up-regulated and 6 spots were down-regulated at 48 hrs of $100\,\mu M$ formaldehyde exposure.

The proteins identified by in-gel digestion and MALDI-TOF MS could be classified into several groups based on their cellular functions and roles in biochemical pathways. Cellular protein quality control system, such as molecular chaperones and ubiquitin-proteasome system, showed notable alterations during formaldehyde-induced cytotoxicity. Several molecular chaperones named Hsp90, Hsp27 and Chaperonin 10-related proteins increased dramatically. Concomitantly, the accumulation of proteasome and ubiquitin carboxyl-terminal esterase occurred after formaldehyde treatment. Many proteins involved in redox regulation of the cell were significantly up-regulated by formaldehyde. Peroxiredoxin 3 plays an important role in eliminating peroxides through the reduction of Reactive Oxygen Species (ROS) via the thioredoxin system[21]. Induction of superoxide dismutase, known to destroy radicals, also reflects increased cellular stress by formaldehyde.

Rho-GDP dissociation inhibitor (GDI)-α was up-regulated in formaldehyde-treated cell. GDI family, consisting of GDI-α, -β, and -γ, is known to regulate actin cytoskeleton-dependent cell functions. GDI-β was suggested to be involved in the airway remodeling of asthma mouse lung tissue[22], and the loss of GDI-α resulted in the progressive impairment of kidney and reproductive organs in mice[23]. Moreover, Rho GDP dissociation inhibitor was reported to play a key role in mitochondrial control of apoptosis[22,23]. Increased expression of these proteins resulted in apoptosis inhibition, consequently promoting uncontrolled growth of the malignant liver cells.

Notably, vinculin was the most interesting among the identified proteins. According to the 2-DE result,

Table 1. Identification of altered protein from human lung epithelial cells following formaldehyde treatment.

Spot no.	Identified protein	Accession no.	Cov %	Matching peptide no	Tr/M.W/pI	Change
1	C-1-tetrahydrofolate synthase, cytoplasmin (C1-THF synthase)	P11586	11	11	102.23/6.9	↗
2	Rho GDP dissociation inhibitor (GDI) alpha	NP_004300	10	40	23.25/5.0	↗
3	CPS1 isoform	AAP84318	10	10	117.10/5.7	↗
4	Carbamoylphosphate synthetase I	BAD74209	10	14	166.00/6.3	↗
5	Vinculin isoform VCL	NP_003364	18	14	117.28/5.8	↗
6	Vinculin	AAH39174	21	17	117.29/5.8	↗
7	Vinculin isoform VCL	NP_003364	18	15	117.28/5.8	↗
8	Heat shock 90 KDa protein 1, beta	NP_031381	21	12	83.59/5.0	↗
9	Helicase-MOI	BAA78691	9	13	221.53/5.5	↘
10	Aldolase A	1ALD	30	9	39.73/8.8	↘
11	Annexin I	NP_000691	44	14	38.92/6.6	↗
12	Annexin A4	P09525	49	16	36.09/5.8	↗
13	Carbonyl reductase 1	NP_001748	57	13	30.64/8.9	↘
14	Ubiquitin carboxyl-terminal esterase L1	NP_004172	53	11	25.15/5.3	↗
15	Heat shock 27 KDa protein 1	NP_001531	37	8	22.82/6.0	↗
16	Proteasome alpha 6 subunit	NP_002782	40	8	27.84/6.3	↗
17	Phosphoglycerate mutase 1 (brain)	AAH62302	34	9	28.92/6.7	↗
18	PSMA4 protein	AAH22817	38	9	29.62/7.7	↗
19	Chain A, Triosephosphate isomerase (Tim) (E.C.5.3.1.1) complexed with 2-phosphoglycolic acid	1HTIA	66	17	26.81/6.5	↗
20	Chain A, Crystal structure of Hgstp1-1[v104] complexed with the Gsh conjugate of (+)-Anti-Bpde	4PGTA	43	8	23.39/5.4	↗
21	Peroxiredoxin 3 isoform b	NP_054817	30	5	26.11/7.1	↗
22	Chain A, Crystal structure of human Dj-1	1J42A	31	6	20.06/6.3	↗
23	Peroxiredoxin 1	NP_002565	72	18	22.32/8.	↘
24	Non-metastatic cells 1, protein (NM23A) expressed in isoform a	NP_937818	53	11	19.86/5.4	↗
25	Chain A, the structure of Holo type human Cu, Zn superoxide dismutase	1HL5A	39	4	16.01/5.7	↗
26	Cofilin 1	NP_005498	36	7	18.71/8.5	↘
27	Chain A, Nucleoside triphosphate, Nucleoside diphosphate Mol_id : 1; molecule : Nucleoside-diphosphate kinase; chain : A, B, C, D, E, F ; Ec : 2.7.4.6	1NUEA	54	7	17.26/8.8	↘
28	Chain A, Cyclophilin A complexed with Cyclosporin A (Nmr,22 structure)	3CYSA	39	9	18.09/8.1	↗
29	Chain A, Cyclophilin A complexed with Cyclosporin A (Nmr,22 structure)	3CYSA	33	6	18.09/8.1	↗
30	Chaperonin 10-related protein	AAC96332	35	5	10.28/9.0	↗

↗: up-regulation, ↘: down-regulation

vinculin was up-regulated in formaldehyde-treated cell by approximately 3 folds. Western blot result was also consistent with the proteomic data. Vinculin is a cytoskeleton protein associated with the cytoplasmic faces of both cell-cell and cell-extracellular matrix adherens-type junctions. It is thought to be implicated in anchoring F-actin to the membrane, and it represents a key element in the transmembrane linkage of the extracellular matrix to the cytoplasmic micro-filament system[24]. The dramatic increase in the vinculin seems to be related with the maintenance of the cell structure in the severely stressed cell by formaldehyde.

Cofilin, known to promote actin depolymerization and inhibit glucocorticoid receptor, was reduced by formaldehyde. Both its actin depolymerization and inhibitory action on the glucocorticoid receptor are dependent on its phosphorylation state.

Annexin, an inflammation related protein, was remarkably increased following formaldehyde treatment. Annexins are characterized as calcium-dependent phospholipid-binding proteins involved in various cellular functions, such as adhesion, exocytosis, and interaction with cytoskeletal proteins and for contribution to the regulation of anti-inflammatory actions of glucocorticoid, cell migration, cell growth and apoptosis[25,26]. Annexin A4 is thought to be involved in membrane trafficking and membrane organization within cells[27].

Cyclophilin is a ubiquitous intracellular protein that binds to the immunosuppressive drug cyclosporine A. Thus, the increase in the cyclophilin by formaldehyde

seems to be related with immunosuppression such as T-cell inhibition[28].

DJ-1 superfamily protein, suggested to play a protective role against neurodegenerative diseases, was also increased in formaldehyde-treated cell[29]. Absorbed formaldehyde is thought to be oxidized to formate and carbon dioxide or possibly incorporated into biological macromolecules via tetrahydrofolate-dependent one-carbon biosynthetic pathways[7,8]. Hence, the increase of C-1 tetrahydrofolate synthase in this study seems to be related with the enhancement of formaldehyde metabolism.

Proteomics provides a powerful application tool for environmental toxicology with the potential to identify novel biomarkers. We used proteomic approaches to identify differentially expressed proteins in human lung epithelial cells by formaldehyde. The identified proteins may be candidates as biomarkers for formaldehyde toxicity in human.

Methods

Human Lung Epithelial Cells and Formaldehyde Treatment

NCI-H292 (human lung epithelial cell) was maintained in RPMI-1640 media with 10% Fetal Bovine Serum (FBS) and 1% penicillin · streptomycin and kept in a humidified 5% CO_2 at 37°C. The NCI-H-292 cells were cultured in a 96-well at a density of 5 $\times 10^4$ cells per well. The cells were then treated with 100 μM formaldehyde for 0, 12, 24 and 48 hrs. 37% formaldehyde solution was purchased from Sigma (USA).

After formaldehyde treatment, the cells were washed and treated with MTT (3-(4, 5-dimethylthiazol-2-yl)-2, 5-diphenyl tetrazolium bromide) to determine cell viability by using MTT assay. After formazan formation by MTT, 100 μL dimethylsulfoxide was added and the absorbance was measured at 570 nm. The determination of cell viability was calculated as [(absorbance of the formaldehyde-treated sample)/(control absorbance)] $\times 100$.

NCI-H292 Cell Prepararion for 2-DE

Harvested NCI-H292 cells were extracted with lysis buffer containing 50 mM Tris HCl (pH 5), 0.1% Triton X-100 and 1 mM PMSF protease inhibitor. After centrifugation the supernatant was collected, and protein concentration was determined using Bradford assay kit. Protein was precipitated with 10% TCA in acetone. The protein pellet was washed with ice-cold acetone at least 5 times in order to remove contaminants.

IEF and 2-DE

For IEF in the first dimension, dried protein samples were dissolved in 500 μL rehydration buffer (7 M urea, 2 M thiourea, 4% CHAPS, 0.5% ampholytes, 100 mM DTT and 0.01% bromophenol blue). The sample solution was applied on immobilized pH 3-10 nonlinear gradient drystrips using an IPG phor system (GE Healthcare Biosciences). Focusing was performed using the following steps: rehydration for 12 hrs, 250 V/100 Vhr, 500 V/500 Vhr, 1,000 V/1,000 Vhr, 8,000 V/38,000 Vhr. After IEF, the individual IPG strips were equilibrated in 6 M urea, 2% SDS, 50 mM Tris-HCl (pH 8.8), 2% DTT and 10% glycerol for 15 min and subsequently incubated in the same buffer for another 15 min after replacing DTT with 2.5% iodoacetamide. Gel was run at 10 mA/gel for 15 min for the initial migration and then 35 mA/gel for 8 hrs[30].

Image Analysis

The gels were visualized using CBB-G250 (Coomassie brilliant blue G-250) staining method. The stained gels were scanned using a UMAX scanner (UMAX Technologies, Plano, TX), and the data were analyzed using Image Master 2D Elite software (GE Healthcare Biosciences).

Protein Digestion and Mass Spectrometric Analysis

Differentially expressed protein spots were excised from the gel. Gel pieces were washed twice with 25 mM ammonium bicarbonate, pH 8.2, 50% v/v acetonitrile (ACN) and then dehydrated by the addition of 100% ACN. 30 ng of trypsin in 25 mM ammonium bicarbonate was added to each gel piece and incubated at 30°C for 16 hrs. The peptide solution was automatically desalted, concentrated and spotted on to the Axima (Kratos, Manchester. UK) MALDI target plate.

Peptide mass fingerprints and Post-Source Decay (PSD) tryptic peptides were generated by matrix assisted laser desorption/ionization-time-of-flight-mass spectrometry (MALDI-TOF-MS) using Ettan MALDI-TOF (GE Healthcare Biosciences). Tryptic peptides derived from protein spots were analyzed and amino acid sequences were deduced using a de novo peptide-sequencing program, PepSeq (Gibbsland). To identify the proteins, sequences were searched against the NCBInr and EST databases using the PROFOUND search program (http://www.rockefeller.edu /labheads/chait/novel_tandem.php) and BLAST.

Western Blot Analysis

After formaldehyde treatment, NCI-H292 cells

were lysed in ice-cold extraction buffer (50 mM Tris-HCl, 0.1% Triton X-100, 1 mM PMSF, pH 7.5) for 30 min at 4°C, and then centrifuged at $12,000 \times g$ for 15 min. Total cellular proteins were denatured and resolved using 12% SDS-PAGE. After the protein was transferred to a polyvinylidene difluoride (PVDF) membrane, it was incubated overnight with the specific antibody at 4°C, and then with the horseradish peroxidase-conjugated anti-mouse IgG for 1 hr. The membranes were visualized using the ECL plus Western-blotting detection system (Santa Cruz Biotechnology).

Acknowledgements

References

1. International Agency for Research on Cancer, On-line database, December (2006).
2. Hester, S. D. *et al*. Formaldehyde-induced gene expression in F344 rat nasal respiratory epithelium. *Toxicology* **187**:13-24 (2003).
3. Hauptmann, M. *et al*. Mortality from solid cancers among workers in formaldehyde industries. *Am J Epidemiol* **159**:1117-1130 (2004).
4. Vaughan, T. L. *et al*. Occupational exposure to formaldehyde and wood dust and nasopharyngeal carcinoma. *Occup Envion Med* **57**:376-384 (2000).
5. Fella, K. *et al*. Use of two-dimensional gel electrophoresis in predictive toxicology: identification of potential early protein biomarkers in chemically induced hepatocarcinogenesis. *Proteomics* **5**:1914-1927 (2005).
6. Tyihak, E. *et al*. Formaldehyde promotes and inhibits the proliferation of cultured tumour and endothelial cells. *Cell Prolif* **34**:135-141 (2001).
7. Marx, C. J., Christoserdova, L. & Lidstrom, M. E. Formaldehyde-detoxifying role of the tetrahydromethanopterin-linked pathway in Methylobacterium extorquens AM1. *Bacteriol* **185**:7160-7168 (2003).
8. Walkup. A. S. & Appling, D. R. Enzymatic characterization of human mitochondrial C1-tetrahydrofolate synthase. *Arch Biochem Biophys* **442**:196-205 (2005).
9. Sanghani, P. C., Robinson, H., Bosron, W. F. & Hurley, T. D. Human glutathione-dependent formaldehyde dehydrogenase. Structures of apo, binary, and inhibitory ternary complexes. *Biochemistry* **41**:10778-10786 (2002).
10. Laouini, D. *et al*. COX-2 inhibition enhances the TH2 immune response to epicutaneous sensitization. *J Allergy Clin Immunol* **116**:390-396 (2005).
11. Takahashi, S. *et al*. Prospective study of clinical symptoms and skin test reactions in medical students exposed to formaldehyde gas. *J Dermatol* **34**:283-289 (2007).
12. Ayaki, H., Lee, M. J., Sumino, K. & Nishino, H. Different cytoprotective effect of antioxidants and change in the iron regulatory system in rodent cells exposed to paraquat or formaldehyde. *Toxicology* **208**:73-79 (2005).
13. Saito, Y., Nishio, K., Yoshida, Y. & Niki, E. Cytotoxic effect of formaldehyde with free radicals via increment of cellular reactive oxygen species. *Toxicology* **210**:235-245 (2005).
14. Quievryn, G. & Zhitkovich, A. Loss of DNA-protein crosslinks from formaldehyde-exposed cells occurs through spontaneous hydrolysis and an active repair process linked to proteosome function. *Carcinogenesis* **21**:1573-1580 (2000).
15. Zhong, W. & Que Hee, S. S. Formaldehyde-induced DNA adducts as biomarkers of in vitro human nasal epithelial cell exposure to formaldehyde. *Mutat Res* **563**:13-24 (2004).
16. Cheng, G. *et al*. Reactions of formaldehyde plus acetaldehyde with deoxyguanosine and DNA: formation of cyclic deoxyguanosine adducts and formalde-hyde crosslinks. *Chem Res Toxicol* **16**:145-152 (2003).
17. Kim, Y. J. *et al*. Genotoxicity and identification of differentially expressed genes of formaldehyde in human jurkat cells. *Mol Cell Toxicol* **1**:230-236 (2005).
18. Speit, G. & Merk, O. Evaluation of mutagenic effects of formaldehyde in vitro: detection of crosslinks and mutations in mouse lymphoma cells. *Mutagenesis* **17**:183-187 (2002).
19. Dowling, V. A. & Sheehan, D. Proteomics as a route to identification of toxicity targets in environmental toxicology. *Proteomics* **6**:5597-5604 (2006).
20. Metz, B. *et al*. Identification of formaldehyde-induced modifications in proteins: reactions with model peptides. *J Bio Chem* **279**:6235-6243 (2004).
21. Wonsey, D. R., Zeller, K.I. & Dang, C.V. The c-Myc target gene PRDX3 is required for mitochondrial homeostasis and neoplastic transformation. *Proc Nat Acad Sci* **99**:6649-6654 (2002).
22. Leffers, H. *et al*. Identification of two human Rho GDP dissociation inhibitor proteins whose overexpression leads to distruption of the actin cytoskeleton. *Exp Cell Res* **209**:165-174 (1993).
23. Togawa. A. *et al*. Progressive impairment of kidneys and reproductive organs in mice lacking Rho GDIα. *Oncogene* **18**:5373-5380 (1999).
24. Hu, K. *et al*. Differential transmission of actin motion within focal adhesion. *Science* **315**:111-115 (2007).
25. Ahmad, M. K., Roderick, J. F. & Mauro, P. An overview of the effects of annexin 1 on cells involved in the inflammatory process. *Mem Inst Oswaldo Cruz* **100**:39-48 (2005).
26. Buckingham, J. C. *et al*. Annexin 1, glucocorticoids and the neuroendocrine immune interface. *Ann N Y Acad Sci* **1088**:396-409 (2006).

27. Fukuoka, S. I., Kern, H., Kazuki, S. R. & Ikeda, Y. Cloning and characterization of ZAP36, an annexin-like, zymogen granule membrane associated protein, in exocrine pancreas. *Biochim Biophys Acta* **1575**: 148-152 (2002).

28. Damsker, J. M., Bukrinsky. M. I. & Constant, S. L. Preferential chemotaxis of activated human CD4＋ T cells by extracellular cyclophilin A. *J Leukoc Biol* **82**: 613-618 (2007).

29. Lee, S. J. *et al*. Crystal structures of human DJ-1 and Escherichia coli Hsp31, which share an evolutionarily conserved domain. *J Biol Chem* **278**:44552-44559 (2003).

30. Kim, Y. K., Yoo, W. I., Lee, S. H. & Lee, M. Y. Proteomic analysis of cadmium-induced protein profiled alterations from marine alga *Nannochloropsis oculata*. *Ecotoxicology* **14**:589-596 (2005).